Mapping roadside nitrogen dioxide concentrations using non-stationary kriging

Serge Antoine Séguret, Laure Malherbe, Gilles Perron

MAPPING ROADSIDE NITROGEN DIOXIDE CONCENTRATIONS USING NON-STATIONARY KRIGING

Serge A. Séguret[1], Laure Malherbe[2*], Gilles Perron[3]

(1) Centre de Géostatistique, Ecole des Mines de Paris, 35, rue Saint-Honoré, 77300 Fontainebleau, France.

(2) Institut National de l'Environnement Industriel et des Risques, INERIS, Parc Technologique ALATA, B. P. N° 2, 60550 Verneuil-en-Halatte, France.

(3) Association pour la Surveillance et l'Etude de la Pollution atmosphérique en Alsace, ASPA, 5, rue de Madrid, 67300 Schiltigheim, France.

**Corresponding author. Tel.: +33 3 44 55 62 18; fax: + 33 3 44 55 68 99*

E-mail address: laure.malherbe@ineris.fr

Abstract

Atmospheric nitrogen dioxide (NO_2) concentrations around a major road in Alsace (France) are estimated on a fine grid using measurements given by passive samplers and a geostatistical approach. Data are referenced to a local coordinate system where (x, y) are respectively the distance from and along the road. They show a strong non-stationarity which does not allow ordinary kriging to be used in the estimation. Therefore a trend is modelled by a combination of exponential and polynomial functions. Experimental residuals are then computed as the differences between measurements and the trend. The idea is to interpolate the residuals at the nodes of the grid, applying kriging methods, and to add them to the trend estimate. Since their variance is not stationary either, an intermediary step is required. It consists in modelling the standard deviation of the residuals as a function of the drift and normalizing the residuals by this model. This defines a new regionalized variable which can be estimated in the framework of stationary geostatistics. Two possible kriging systems are tested, depending on the fitted variogram model: in the first one, a pure nugget effect (white noise) is used, in which case the best linear estimator of NO_2 concentration is the trend model; in the second one, a structured exponential variogram is adjusted. This case study shows that non-stationarity may not only characterize the raw variable but can

also affect the variance of a phenomenon. It illustrates the interest of modelling it so as to improve the experimental variogram, fit an acceptable variogram model and compute the variance of the estimation error even if the estimator is reduced to a simple regression function.

Keywords: geostatistics, non-stationarity, trend estimation, standard deviation model, universal kriging

1. Introduction

Air pollution mapping is a valuable tool for assessing population long-term exposure and informing the public about the spatial distribution of outdoor concentrations. At the regulatory level, calculation of concentration maps is prompted by the European daughter directives on ambient air quality assessment (1999/30/ EC, 2000/69/ EC, 2002/3/ EC).

In France geostatistical methods have been receiving particular attention for several years and are now commonly used by the French air quality monitoring organizations. They are mostly applied for mapping background concentrations at the city or regional scale so as to fulfill the regulatory recommendations. Roadside pollution is equally a matter of concern as regards people exposure and has been the subject of many investigations (Gilbert, 2003, Kodama, 2001, Roorda-Knape, 1999). However, the difficulty in such cases is that concentration usually shows a strong drift (it decreases with distance from the source), which makes the classical methods of stationary geostatistics like ordinary kriging or cokriging unsuitable.

Deletraz and Dabos (2001) tested different interpolating methods in order to map the environmental impact (expressed as NO_2 deposition) of a road in a mountainous region and opted for a multiple regression estimator using the inverse distance from the road and the logarithm of roughness as explicative variables. The regression model explains 87% of the deposition variability. Unlike the geostatistical method explored hereafter, it does not take the residual variability into account. Briggs et al. (2000) also proposed a regression mapping technique to model the spatial patterns of traffic-related pollution. The developed model is a linear combination of variables derived from traffic counts, land cover and altitude.

Several studies show the relevance of geostatistics to treat non-stationary problems in the vicinity of chemical or contaminating sources. Figueira et al. (1999) applied kriging with external drift for estimating soil salinity in a coastal land strip. The logarithm of the distance from the coast was used as an auxiliary variable. The results were compared with those of ordinary kriging. They attested the efficiency of the

external drift. Saito and Goovaerts (2001) applied different techniques based on kriging to estimate lead soil concentrations around a former smelter in Dallas. In particular they modelled a trend by a linear combination of log(d) and $\Delta\theta$, d being the distance from the smelter and $\Delta\theta$ the deviation from the main wind direction. Then they worked with residuals obtained from the difference between measurements and the trend estimates.

In this methodology-oriented study we propose to perform kriging of residuals from a global trend model in order to estimate NO_2 roadside concentrations in the Thur Vosges Valley in Alsace, France.

Concentration data are derived from passive diffusion tube measurements performed 3 meters above the ground at 39 sites around a major road, (Fig. 1-A). The aim of the measurement campaign, which took place in summer 2001, was to assess the environmental impact of traffic. Therefore the samplers were located in places supposed to be strictly under the influence of road emissions. Most tubes were positioned on transepts and situated 1 m, 2 m, 50 m, 200 m, 400 m far from the road. Similar measurements were also conducted in winter. However, the present article focuses on summer average concentrations, calculated from 6 fortnightly records. Results for winter are mentioned only if they present significant differences with summer. The road is 20 km long. To simplify its width has been set to zero as it is not precisely known.

Among all the auxiliary variables (land use, emission inventory, population density …) distance to the road and elevation appear to be explanatory of NO_2 concentration, as indicates a Factorial Component Analysis. Now, the elevation is strongly correlated with distance along the road (curvilinear abscissa) (see Fig.1-B). Consequently NO_2 concentrations are expressed in a coordinate system where (x, y) are distances from and along the road, respectively (Fig. 1-C). By this way elevation is implicitly taken into account.

Data show a clear tendency of NO_2 concentration to decrease with distance from the road, indicating the non-stationary nature of the pollution phenomenon. In that context a mapping methodology based on estimating the trend is suggested.

In what follows, concentration measurements are considered as the realization of a random function $NO_2(x,y)$. The estimation involves four stages.

1. At any point (x,y), NO_2 is written as the sum of a trend m(x,y) providing the general pattern of pollution along and across the road, and a random residual: $NO_2(x,y)=m(x,y)+R(x,y)$
   Therefore this first step consists in adjusting a trend model on the concentration data.
2. As the variance of the residuals depends on their value (non stationary variance), those residuals have to be normalized so that classical kriging methods can be applied. For this purpose their standard deviation is modelled by a function $\sigma(x,y)$.
3. The experimental variogram of the normalized residuals $NR(x,y)=R(x,y)/\sigma(x,y)$ is calculated to describe the spatial variability of concentration fluctuations around the trend and a variogram model is fitted.
4. A simple kriging system is solved to estimate NR(x,y) at the nodes of a 250m x 250m mesh grid. Finally the estimator of $NO_2(x,y)$ is built :

$$NO_2^*(x,y) = \sigma(x,y)NR^*(x,y) + m(x,y)$$

After presenting each stage, we conclude by a discussion where :

- the results are interpreted;
- other possible kriging systems are considered, depending on the confidence given to the trend estimate.

2. Modelling the trend

As a preamble, let us define the notion of non-stationarity : a regionalized phenomenon, namely a physical phenomenon stretching out in space and represented by a function Z, is stationary if its mean m(p) and its covariance cov[Z(p),Z(p+h)] are independent of the location of point p.

Fig. 2-A represents the projection of concentrations on a plane perpendicular to the road. Two main observations can be made: 1) NO_2 concentration decreases sharply with distance from the road, indicating the non-stationary nature of the phenomenon; 2) there is no significant dissymmetry between the left and right sides of the road. The first remark involves trend modelling, the second one allows us to handle the left and right sides together, increasing the total number of available data in a class and hence, the accuracy of the model.

A difficult task is now to give a proper analytical form to the trend.

- For a given $y = y_j$, i.e. when concentration variations are examined perpendicularly to the road, optimality in the least square sense is obtained in the frame of a bi-exponential function of x :

$$m(x,y_j) = a(y_j)\, e^{-\frac{|x|}{s_1}} + b(y_j) e^{-\frac{|x|}{s_2}} \quad [1]$$

with $(s_1, s_2) = (18, 550)$. For distances from the road greater than 1600 meters the drift can be considered as zero. The average concentrations and their interpolated values by function (1) are represented in Fig. 2-B.

In winter $(s_1, s_2) = (14, 940)$. Concentrations are distributed following a different pattern, and become zero at more than 3000 meters from the road. Such a difference with summer can be explained by climatology, changes in the emissions and photochemical consumption of nitrogen oxide in summer. Such observations are consistent with what Monn et al. (1997) already noticed.

- For a given $x = x_i$, i.e. when concentration variations are examined parallel to the road, optimality in the least square sense is obtained in the frame of a linear function of y (Fig. 2-C) :

$$m(x_i,y) = c(x_i)\, y + d(x_i) \quad [2]$$

- Combining formulas (1) and (2) leads to the trend model :

$$m(x,y) = c_0 + (c_1 y + c_2)\, e^{-\frac{|x|}{s_1}} + (c_3 y + c_4) e^{-\frac{|x|}{s_2}} \quad [3]$$

The constant c_0 is introduced so that the trend is not necessarily zero for distances from the road greater than 1600 meters ; the factors s_1 and s_2 are fixed once and for all; the coefficients c_0 to c_4 are obtained by a global regression on the 39 measurements. The trend is represented in three dimensions (Fig. 3-A) and by isovalues (Fig 3-B).

Results are different for each season. For exemple, c_0 is equal to 0.3 µg m^{-3} in summer and 3.5 µg m^{-3} in winter.

Most measurements are located at distances to the road less than 400 meters. Beyond that, the trend model is not conditioned by experimental data and only determined by the mathematical properties of the exponential functions. To prevent improper extrapolation, the use of m(x,y) is restricted to x values below 500 meters on both sides of the road ($|x|<500$ m).

3. Non-stationarity of the variance

Let *u* be the coordinate vector (x,y). Using the trend model (3) the residuals R(u) are calculated at the measurement points :

$$R(u) = NO2(u) - m(u) \quad [4]$$

Those residuals are plotted as a function of m(u) in Fig. 4-A. As expected they fluctuate around 0 but the amplitude of the fluctuations increases with m(u), suggesting that the variance of the residuals is not stationary. Therefore this variance has to be modelled too. The trend values calculated at the sampling points are gathered in six different classes and for each class the standard deviation of the residuals is computed. A power function of m(u) is then adjusted (Fig. 4-B) :

$$\sigma(u) = d\ m(u)^p \quad [5]$$

The parameters d and p are equal to 0.261 and 0.879 respectively (d=0.015 and p=1.57 in winter).

4. Variograms

To get stationarity the residuals are normalized :

$$NR(u) = \frac{R(u)}{\sigma(u)} \quad [6]$$

Such an operation is possible because σ(u) is strictly positive in the domain under study.

Is this normalization (6) really necessary ? The transverse semivariogram (i.e. perpendicular to the road) of R(u) is plotted in Fig. 5-A : the large fluctuations are mainly explained by the contrast of variability between the measurements close to the road and the other concentration measurements. If the non-stationarity of the variance is ignored and the residuals are not normalized then the variance assigned to the first set of measurements is too low and the variance assigned to the second one is too high. Normalization makes it possible to homogenize residuals and is essential to go further in the analysis.

When calculated on NR(u), the transverse variogram is significantly improved (Fig. 5-B). The longitudinal variogram (i.e. along the road, Fig. 5-C) has a cyclic aspect due to the alternation of higher (about 50 µg m^{-3}) and lower (about 40 µg m^{-3}) values for samplers located at distances less than 2 meters from the road. The housing type may explain such concentration variations but additional information need to be collected to confirm such an hypothesis. The first point of the longitudinal variogram is calculated with only ten pairs of data whereas the second one is computed with 118 pairs. Whether or not

178 the first point is taken into account and the transversal or longitudinal variogram is assigned with a
179 structure, two approaches are examined :

180 - the variogram is considered as not being structured in any of the directions (white noise) : it is
181 modelled by a pure nugget effect equal to the variance of NR(u) : C(0)=1.13.
182 - a structure is detected and described by the sum of a nugget effect and an exponential model with a
183 geometrical anisotropy of ranges 1450 m in the x-direction and 10000 m in the y –direction
184 (respectively 80 m and 2200 m in winter).

185

186 ## 5. Estimation

187

188 Whatever the approach, let C(h) be the covariance of NR(u). It is linked to the stationary variogram by
189 the relationship :

190 $$C(h) = C(0) - \gamma(h)$$

191 The normalized residuals are estimated at the nodes $u_0 = (x_0, y_0)$ of a grid by a linear combination of the n
192 = 39 concentration measurements :

$$NR^*(u_0) = \sum_{\alpha=1}^{n} \lambda_\alpha \, NR(u_\alpha) \qquad [7\text{-a}]$$

193 The kriging weights λ_α are the solution of a simple kriging system :

$$\sum_{\alpha=1}^{n} \lambda_\alpha \, C_{\alpha\beta} = C_{\beta 0} \qquad \forall \beta : 1, n \qquad [7\text{-b}]$$

194 where $C_{\alpha\beta}$ (resp. $C_{\beta 0}$) stands for the covariance between measurements taken in u_α and u_β (resp. u_β and
195 u_0).

196 The estimator of $NO_2(u_0)$ is obtained setting :

$$NO_2^*(u_0) = \sigma(u_0) \, NR^*(u_0) + m(u_0) \qquad [7\text{-c}]$$

197 where $m(u_0)$ and $\sigma(u_0)$ are given by (3) and (5).

198 The variance of the estimation error is :

$$\sigma^2_{NO_2}(u_0) = \sigma^2(u_0) \, (C(0) - \sum_{\alpha=1}^{n} \lambda^\alpha C_{\alpha 0}) \qquad [7\text{-d}]$$

199 When the covariance C(h) is described by a pure nugget effect, the weights minimizing (7-d) are all zero
200 and the estimation is reduced to :

$$NO_2^*(u_0) = m(u_0) \quad [8\text{-a}]$$

This result is actually well-known : kriging with a nugget covariance is strictly equivalent to estimating the trend. Here the trend has been obtained by a mean-square regression. At each node of the grid, the estimation variance is then :

$$\sigma^2_{NO_2}(u_0) = \sigma^2(u_0)\, C(0) \quad [8\text{-b}]$$

As C(0) is close to 1, σ_{NO2} is nearly equal to the non-normalized residues standard deviation model σ given by (5).

Fig. 6-A shows the estimation of concentrations using an exponential covariance. Comparing it with the trend representation (Fig. 3-B) makes it evident how the isolines get distorted to fit the experimental values. Such a comparison points up the advantage of kriging over a mean-square regression and the interest of modelling the variogram when possible. The estimation standard deviation for that kriging is displayed in Fig. 6-B. Compared to the one associated with regression (Fig. 6-C) it is lower around the data points.

6. Conclusion and discussion

Through the analysis of a case example, a methodology is proposed for elaborating concentration maps in presence of a spatial trend. Though the limited number of data did not facilitate the interpretation of the variogram (see section 4), our aim was to point out the interest of modelling non-stationarity when it affects a variable and its variance. Here we discuss the choices we made for calculating the variogram and defining a model.

6.1 Interpretation of the results

The variogram $\gamma(h)$ is computed with residuals derived from a trend estimate, which necessarily introduces a bias (Matheron, 1970). As a consequence, the real underlying variogram, assuming it is structured, can be either masked or deformed, depending on the representativity of the data. Quantifying the impact of the number of samplers on the quality of the trend estimate is not easy. However the estimation standard deviation map for a nugget covariance model may be a useful tool for evaluating kriging results (Fig. 6-C). On the road axis the standard deviation is 8 μgm^{-3} at y=5 km. Then it decreases sharply till it reaches 1 at y = 20 km and x = ±500m. If the standard deviation is not to be larger than 3.5 μgm^{-3} for example, then only the area where this condition is met should be selected for representing

concentrations, whereas estimates near the road are ignored (hatched region in Fig. 6-C). This interpretation of the kriging standard deviation map is strengthened by sensitivity tests consisting in estimating m(x, y) with restricted data sets. According to such tests, the trend estimate was sensitive to data located less than 2 m from the road. For longer distances the coefficients c_0 to c_4 of formula (3) did not change significantly if 4 or 5 measurements were removed randomly. The poorer quality of estimation near the road is to be expected since concentrations, and hence the estimation variances, are higher there. To improve it, more measurements are required.

The kriging standard deviation map for an exponential covariance model (Fig. 6-B) can be studied in the same way. Regions respecting the quality criterion, expressed as a maximal value for kriging standard deviation, can be selected as previously.

6.2 Using the IRF-k theory ?

A drawback of the proposed methodology is that the final NO_2 concentration estimate closely depends on the mean-square trend estimate. To weaken this dependency relationship a more elaborated kriging system might be used. Actually two different systems could be envisaged :

- universal kriging of NO_2 (Appendix 1) : an affine function of the trend m(u) is reestimated;
- a more general universal kriging of NO_2 (Appendix 2): all the coefficients of the trend are reestimated.

Whatever the chosen method, all the systems proceed from the non stationary approach called Universal Kriging (Matheron, 1969) and do not solve the problem of the bias of the variogram which has been previously mentioned.

The theory of the Intrinsic Random Functions of order k (IRF-k) (Matheron, 1971) was developed to answer that problem. A synthetic description can be found in Chilès and Delfiner (1999). To summarize, we can say that this theory implies fitting most part of the phenomenon by all possible linear combination of polynomials having a given degree k, the variability of the residuals being modelled by a Generalized Covariance. This method is useful when polynomials can explain the large-scale spatial behaviour of the phenomenon under study. Is it the case here? Fig. 7 represents the averaged concentrations projected on a plane perpendicular to the road, and their regression by polynomials. To obtain an acceptable approximation, we need to use at least all the degrees of x up to 4. This implies modelling the trend using a term in yx^4 relevant of an IRF-5. As the set of polynomials must be complete, in order to ensure the

regularity of the kriging system, the trend must then be developed on 21 monomials with as much multiplicative coefficients to be calculated. This is not reasonable.

Universal kriging seems therefore to be an effective way of handling the problem of double non-stationarity in mean and variance. It is based on hypotheses consistent with the spatial pollution pattern. Besides this methodology does not involve complex mathematical developments and is suitable for regular use, in compliance with regulatory requirements.

Appendix 1 : Universal Kriging of NO_2

A linear system is built where a linear function of the trend m(u) is locally estimated by kriging. $NO_2(u)$ is consequently expressed as :

$$NO_2(u) = \sigma(u)\, NR(u) + a_0\ m(u) + a_1 \qquad [A1\text{-}1]$$

where a_0 and a_1 are unknown and m(u) is the trend previously obtained by least square regression. The specificity of the present application is a non stationary covariance :

$$Cov(NO_2(u),NO_2(v)) = \sigma(u)\ \sigma(v)\ C(v\text{-}u) \qquad [A1\text{-}2]$$

At any node u_0 of the estimation grid, the estimator is a linear combination of measurements taken at the points u_α :

$$NO_2{}^*(u_0) = \sum_{\alpha=1}^{n} \lambda_\alpha\ NO_2(u_\alpha) \qquad [A1\text{-}3]$$

The weights λ_α are solutions of the following system :

$$\sum_{\alpha=1}^{n} \lambda_\alpha \sigma(u_\alpha)\ \sigma(u_\beta)\ C_{\alpha\beta} + \mu_0 + \mu_1\ m(u_\beta) = \sigma(u_\beta)\ \sigma(u_0)\ C_{\beta 0} \qquad \forall \beta : 1, n \qquad [A1\text{-}4]$$

$$\sum_{\alpha=1}^{n} \lambda_\alpha = 1 \qquad [A1\text{-}5]$$

$$\sum_{\alpha=1}^{n} \lambda_\alpha m(u_\alpha) = m(u_0) \qquad [A1\text{-}6]$$

The estimation error is defined as the difference $NO_2{}^*(u_0)$-$NO_2(u_0)$. Its variance is given by :

$$\sigma^2_{NO_2}(u_0) = \sigma^2(u_0)\ C(0) - \sum_{\alpha=1}^{n} \lambda^\alpha \sigma(u_\alpha)\ \sigma(u_0)\ C_{\alpha 0} - \mu_0 - \mu_1\ m(u_0) \qquad [A1\text{-}7]$$

Coefficients μ_0 et μ_1 are Lagrange parameters imposed by the universality conditions (A1-5) and (A1-6). Equations (A1-4) to (A1-6) make a classical Universal Kriging system which has the distinctive feature of using a non-stationary covariance $\sigma(u)\sigma(u+h)C(h)$. This system is reversible and has a unique solution since the covariance $\sigma(u)\sigma(u+h)C(h)$ is positive definite like C(h). The data are NO_2 measurements (and not the normalized residuals NR). It must be useful to use a moving neighborhood with at least 10 measurements around the node u_0 where the estimator is calculated.

Appendix 2 : more general Universal Kriging of NO_2

A linear system is built where the coefficients c_0 to c_4 of the trend m(u) are locally estimated by kriging.

If we put :

$\{X^l, l=1 \text{ to } 5\} = \{1, e^{-\frac{|x|}{s_1}}, e^{-\frac{|x|}{s_2}}, y\, e^{-\frac{|x|}{s_1}}, y\, e^{-\frac{|x|}{s_2}}\}$

the kriging system becomes :

$$\sum_{\alpha=1}^{n} \lambda_\alpha \sigma(u_\alpha)\, \sigma(u_\beta)\, C_{\alpha\beta} + \sum_{l=1}^{5} \mu_l X^l(u_\beta) = \sigma(u_\beta)\, \sigma(u_0)\, C_{\beta 0} \qquad \forall \beta : 1, n \qquad \text{[A2-1]}$$

$$\sum_{\alpha=1}^{n} \lambda_\alpha X^l(u_\alpha) = X^l(u_0) \qquad \forall\, l : 1, 5 \qquad \text{[A2-2]}$$

and the variance of the error is :

$$\sigma^2_{NO_2}(u_0) = \sigma^2(u_0)\, C(0) - \sum_{\alpha=1}^{n} \lambda^\alpha \sigma(u_\alpha)\, \sigma(u_0)\, C_{\alpha 0} - \sum_{l=1}^{5} \mu_l\, X^l(u_0) \qquad \text{[A2-2]}$$

Those expressions use five Lagrange multipliers μ_l. As previously, it is advised to use a moving neighborhood. The selected data must not lie on a line.

Acknowledgements

Data were provided by the French Association for the Surveillance and Study of the Atmospheric Pollution in Alsace (ASPA). The complete study, and especially a detailed description of the data, can be found in Seguret (2003). The geostatistical calculations were made with the software Isatis (Géovariances, www.geovariances.fr). Funding was provided by the French Ministry of Ecology and Sustainable Development. The authors would like to thank Mrs Françoise Poirier and Dr Jean-Paul Chilès, from the Centre de Géostatistique of Fontainebleau, who corrected their English and usefully commented a draft version of the manuscript.

References

Briggs, D.J., Hoogh (de), C., Gulliver, J., Wills, J., Elliott, P., Kingham, S., Smallbone, K., 2000. A regression-based method for mapping traffic-related air pollution: application and testing in four contrasting urban environments. The Science of the Total Environment, 253, 151-167.

Chilès, J.-P., Delfiner, P. 1999. Geostatistics. Modeling Spatial Uncertainty. Wiley, New York.

Deletraz, G., Dabos, P. 2001. Modélisation statistique de la pollution azotée à proximité d'un axe routier et évaluation des incidences sur l'environnement. Colloque Risques – octobre 2001, Besançon.

Council Directive 1999/30/EC of 22 April 1999 relating to limit values for sulphur dioxide, nitrogen dioxide and oxides of nitrogen, particulate matter and lead in ambient air.

Directive 2000/69/EC of the European Parliament and of the Council of 16 November 2000 relating to limit values for benzene and carbon monoxide in ambient air.

Directive 2002/3/EC of the European Parliament and of the Council of 12 February 2002 relating to ozone in ambient air.

Figueira, R., Sousa, A.J., Pacheco, A.M.G., Catarino, F. 1999. Saline variability at ground level after kriging data from *Ramalina* app. Biomonitors. The Science of the Total Environment, 232, 3-11.

Gilbert, N.L., Woodhouse, S., Stieb, D.M., Brook, J.R., 2003. Ambient nitrogen dioxide and distance from a major highway. The Science of the Total Environment, 312, 43-46.

Kodama, Y., Arashidani, K., Tokui, N., Kawamoto, T., Matsuno, K., Kunugita, N., Minakawa, N., 2002. Environmental NO2 concentration and exposure in daily life along main roads in Tokyo. Environmental Research, Section A, 89, 236-244.

Matheron, G., 1969. Le Krigeage Universel. Cahiers du Centre de Morphologie Mathématique de Fontainebleau, Fascicule 1, Ecole des Mines de Paris.

Matheron, G. 1970. La Théorie des Variables Régionalisées et ses Applications. Cahiers du Centre de Morphologie Mathématique de Fontainebleau, Fasc. 5, Ecole des Mines de Paris. Translation (1971) : The Theory of Regionalized Variables and Its applications.

Matheron, G. 1971. La Théorie des Fonctions Aléatoires Intrinsèques Généralisées. Note Géostatistique No 117. Technical Report N-252, Centre de Géostatistique, Fontainebleau, France.

Monn, Ch., Carabias, V., Junker, M., Waeber, R., Karrer, M., Wanner, H.U. 1997. Small-scale spatial variability of particulate matter <10 μm (PM_{10}) and nitrogen dioxide. Atmospheric Environment, 31 (15), 2243-2247.

Roorda-Knape, M., Janssen, N.A.H., Hartog (de), J., Van Vliet, P.H.N., Harssema, H., Brunekreef, B., 1999. Traffic related air pollution in city districts near motorways, The Science of the Total Environment, 235, 339-341.

Saito, H., Goovaerts, P., 2001. Accounting for source location and transport direction into geostatistical prediction of contaminants. Environmental Science and Technology, 35, 4823-4829.

Séguret, S.A., 2003. Estimation du dioxyde d'azote routier dans la vallée de la Thur. Technical Report N-1/03/G available on pdf file at http://www.lcsqa.org.

Figure captions

Fig. 1 : (A) Road representation in the original geographical system. The red points stand for the 39 measurement points, 33 of which lie on transepts T1 to T6.

(B) Correlation cloud between altitude and measurement distance along the road (curvilinear abscissa).

(C) Location of measurements in the local reference system.

Fig. 2 : (A) Projection of the measurement data onto a plane perpendicular to the road (only data located on transepts have been projected). Black points represent the average concentrations for different distance classes (|x|=1m, 2m, 50m, 200m and 400m apart from the road).

(B) Average concentrations for the considered distance classes and adjustment of a combination of two exponential functions.

(C) Concentration variations along the road (i.e. along y) for each |x|-distance class and their approximation by linear functions.

Fig. 3 : (A, B) Graphic representation of the trend m(x,y) in perspective (A) and in isolines (B). The red and black isolines are 10 $\mu g\ m^{-3}$and 2 $\mu g\ m^{-3}$ distant from each other, respectively.

Fig. 4 : (A) Residuals R(u) = NO_2(u) - m(u) as a function of the trend m(u). u = (x,y) is the coordinate vector in the local reference frame. R(u) fluctuations around 0 grow with m(u). (B) R(u) standard deviations for each m(u) value class and adjustment of a model written as d $m(u)^p$, with d=0.261 and p=0.879.

Fig. 5 : (A) Experimental variogram of the residuals R(u) in the transverse direction before standardization. (B) Experimental variogram of the standardized residuals R(u) in the transverse direction. The number of pairs participating to the calculation of each point are indicated on the graph. Two types of models have been fitted: a pure nugget model (in blue) and a nugget+exponential

anisotropic model with a range of 1.45 km along x and 10 km along y. (C) Variogram of the standardized residuals along the road.

Fig. 6 : (A) Nitrogen dioxide concentration obtained by simple kriging of the standardized residuals, using a structured variogram model. Size of the data points is proportional to the measurement values. (B) Kriging standard deviation for the above calculated map. (C) Kriging standard deviation for a pure nugget variogram model. It is almost equal to $\sigma(x,y)$ and can be regarded as the error standard deviation for the trend estimation. In the red hatched area the standard deviation is greater than 3.5.

Fig. 7 : NO_2 concentrations across the road (green dashed curve) and their approximation by 2^{nd} to 4^{th} order polynomial functions (solid curves).

401 **Colour illustrations**

402

A

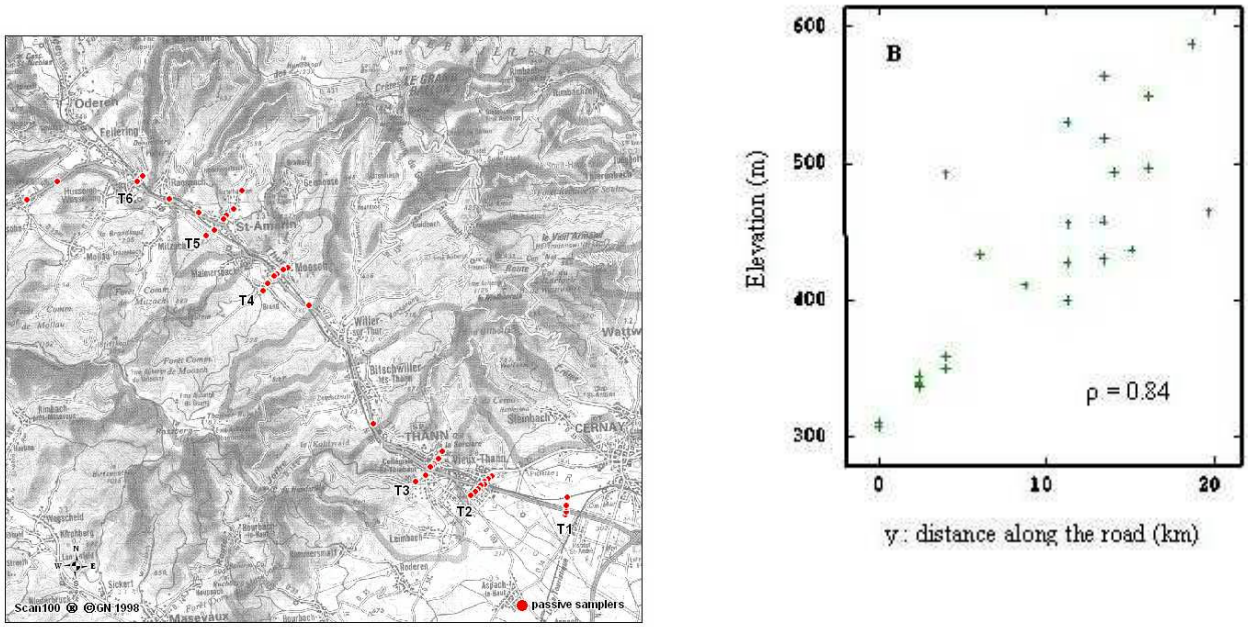

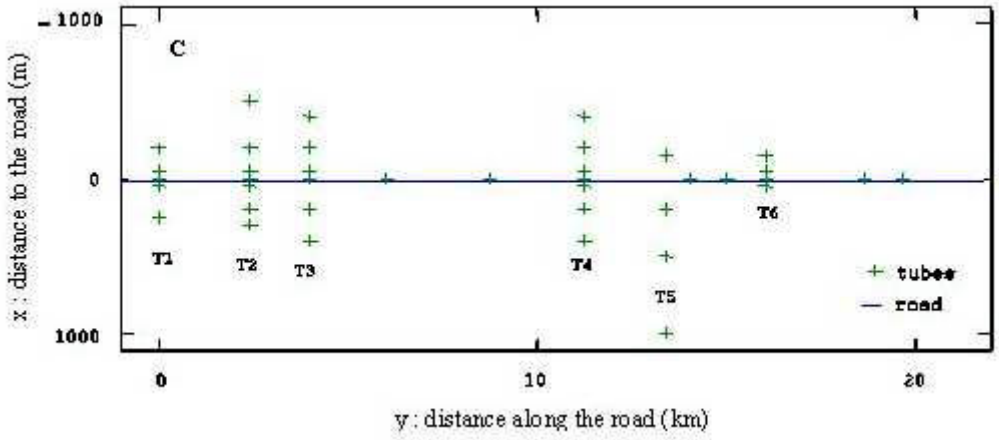

403

404 Fig. 1

405

406

407

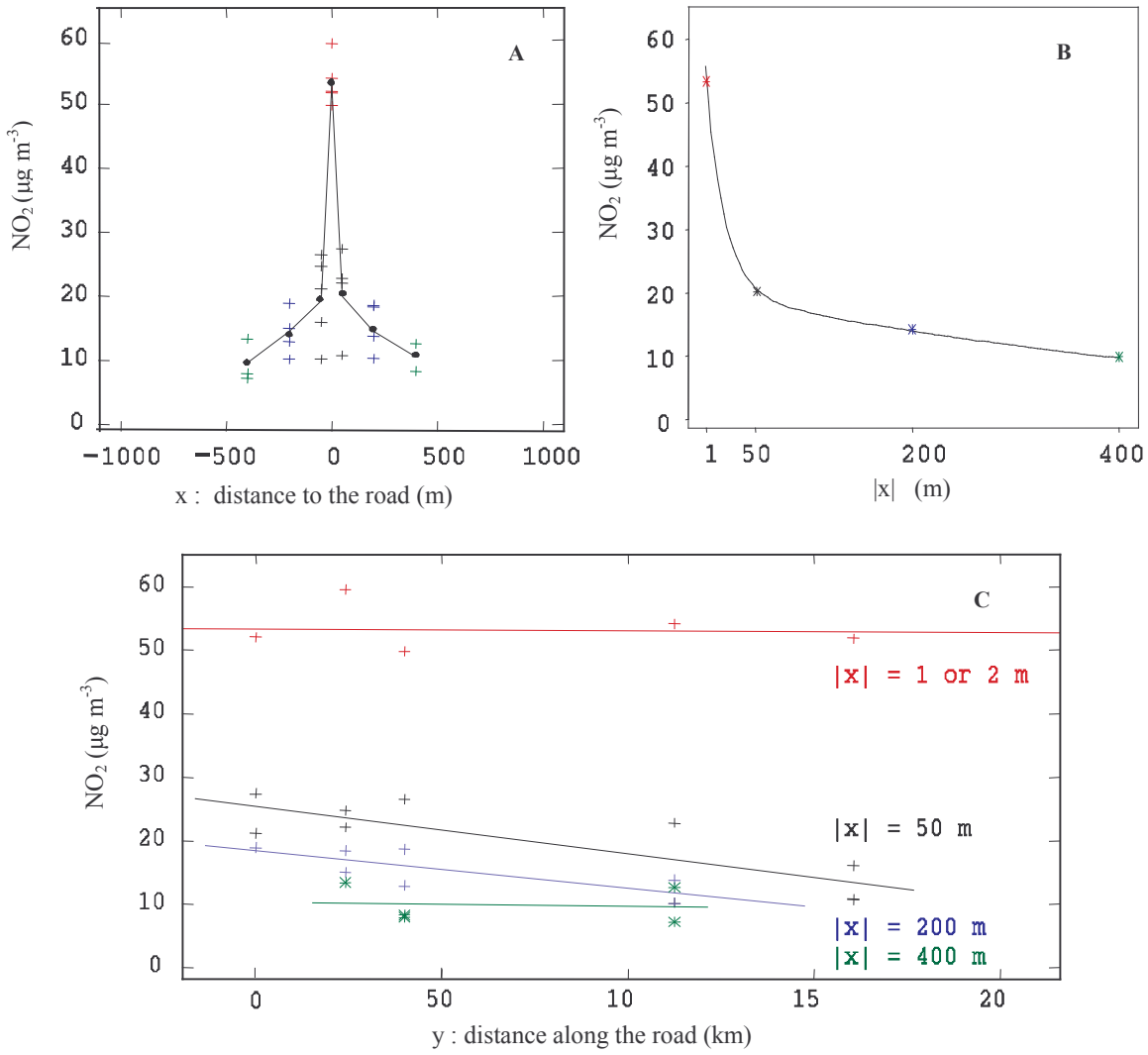

408

409 Fig. 2

410

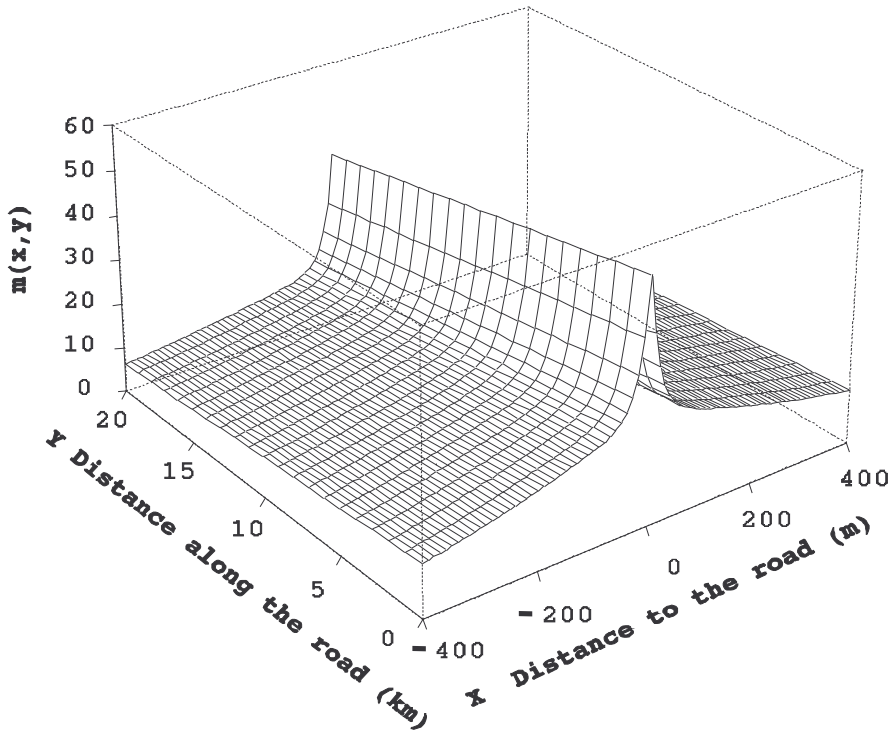

A

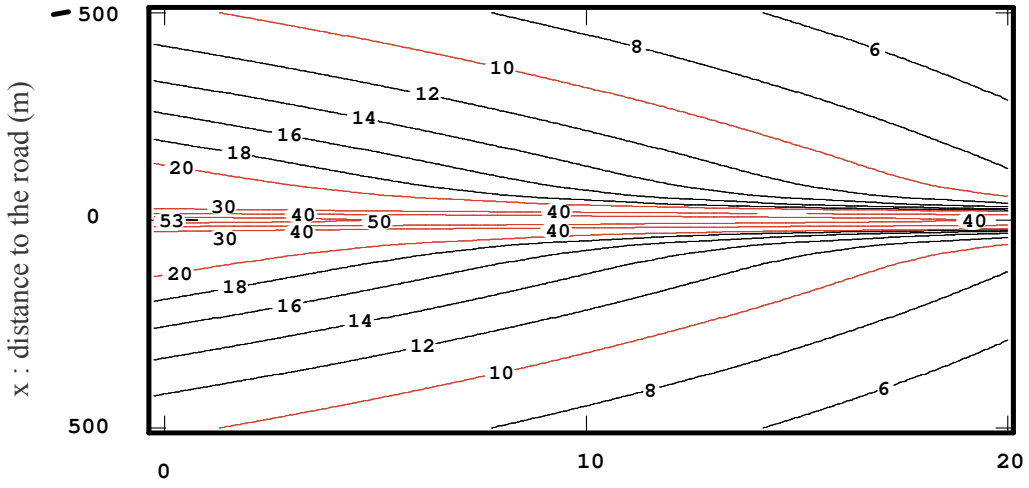

B

411 Fig. 3

412

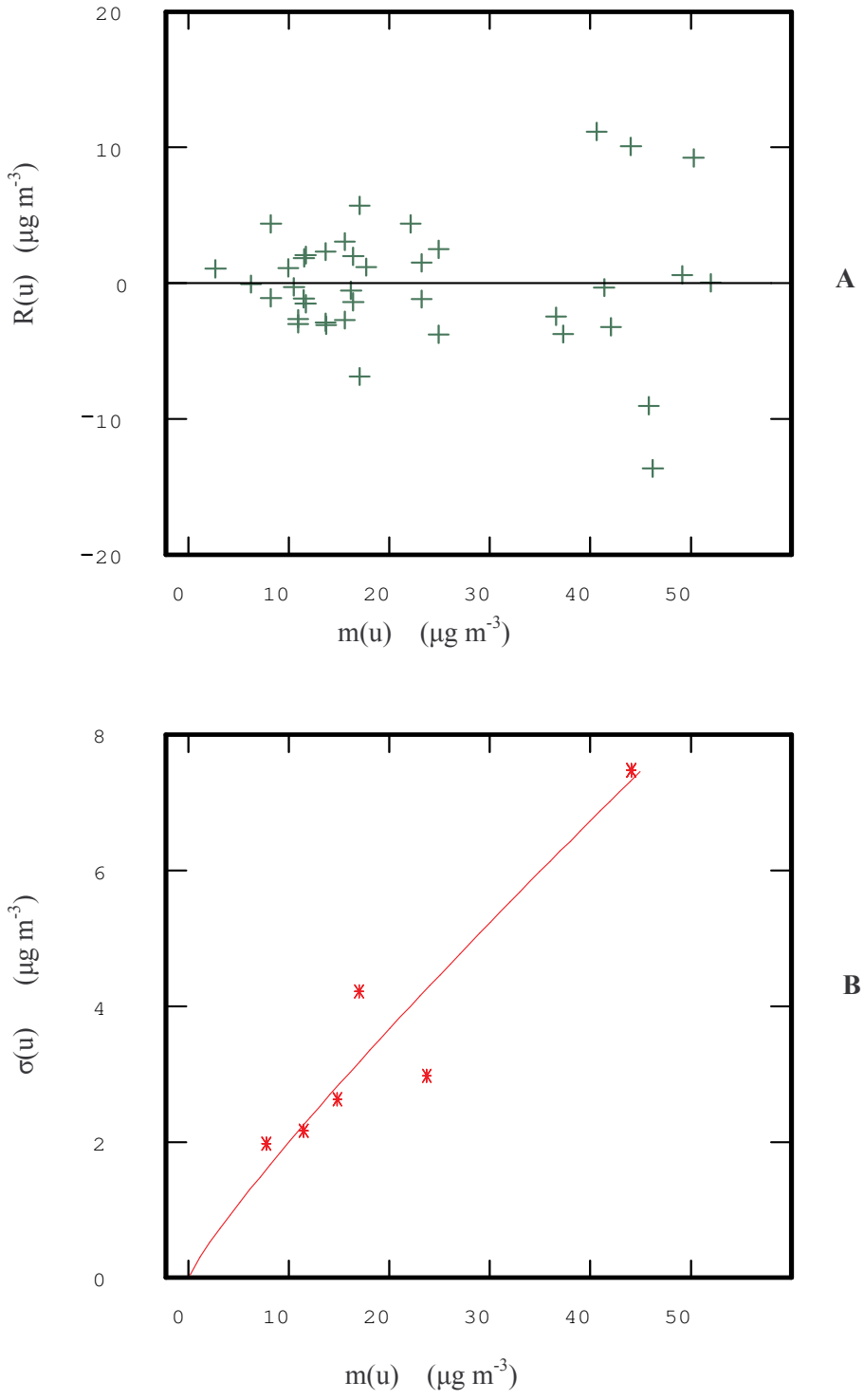
20
10
0
−10
−20
R(u) (µg m-3)
0
10
20
30
40
50
m(u) (µg m-3)
A
8
6
4
2
0
σ(u) (µg m-3)
0
10
20
30
40
50
m(u) (µg m-3)
B

413 Fig. 4

414

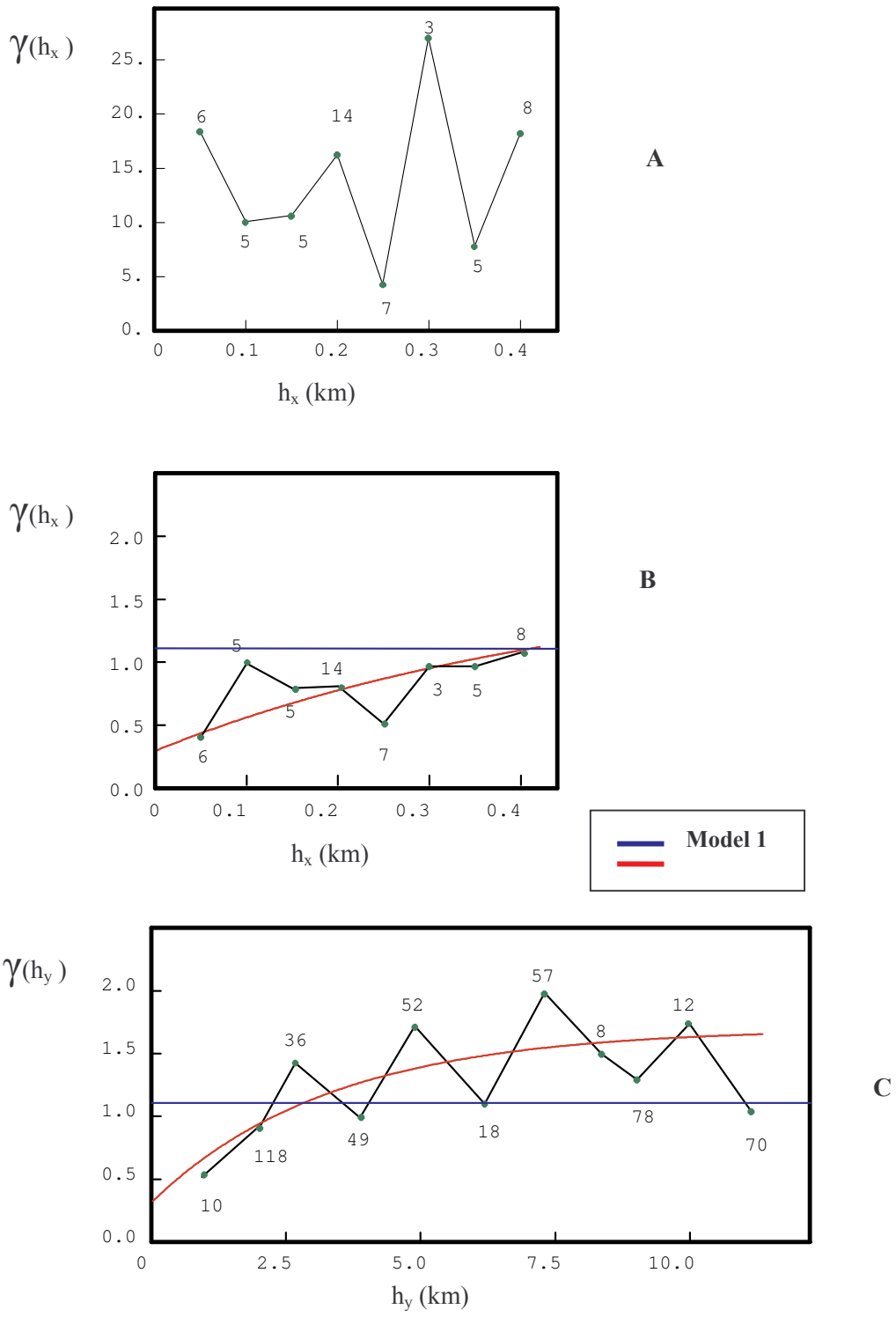
γ(hx)
25.
20.
15.
10.
5.
0.
6
5
5
14
7
3
5
8
0
0.1
0.2
0.3
0.4
hx (km)
A
γ(hx)
2.0
1.5
1.0
0.5
0.0
5
6
5
14
7
3
5
8
0
0.1
0.2
0.3
0.4
hx (km)
B
Model 1
γ(hy)
2.0
1.5
1.0
0.5
0.0
10
118
36
49
52
18
57
8
78
12
70
0
2.5
5.0
7.5
10.0
hy (km)
C

415 Fig. 5

416

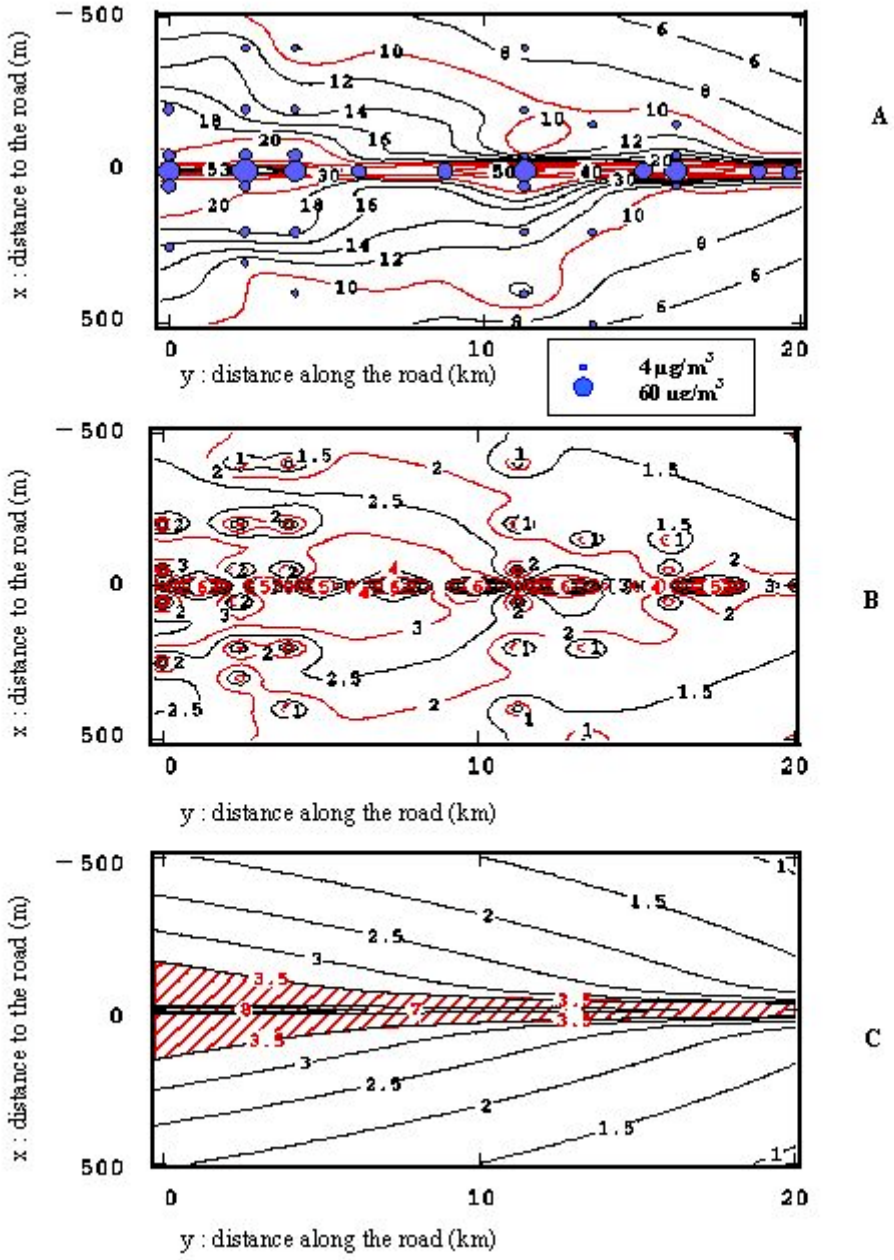
A
B
C
x : distance to the road (m)
y : distance along the road (km)
− 500
0
500
0
10
20
4 µg/m3
60 µg/m3

417 Fig. 6

418

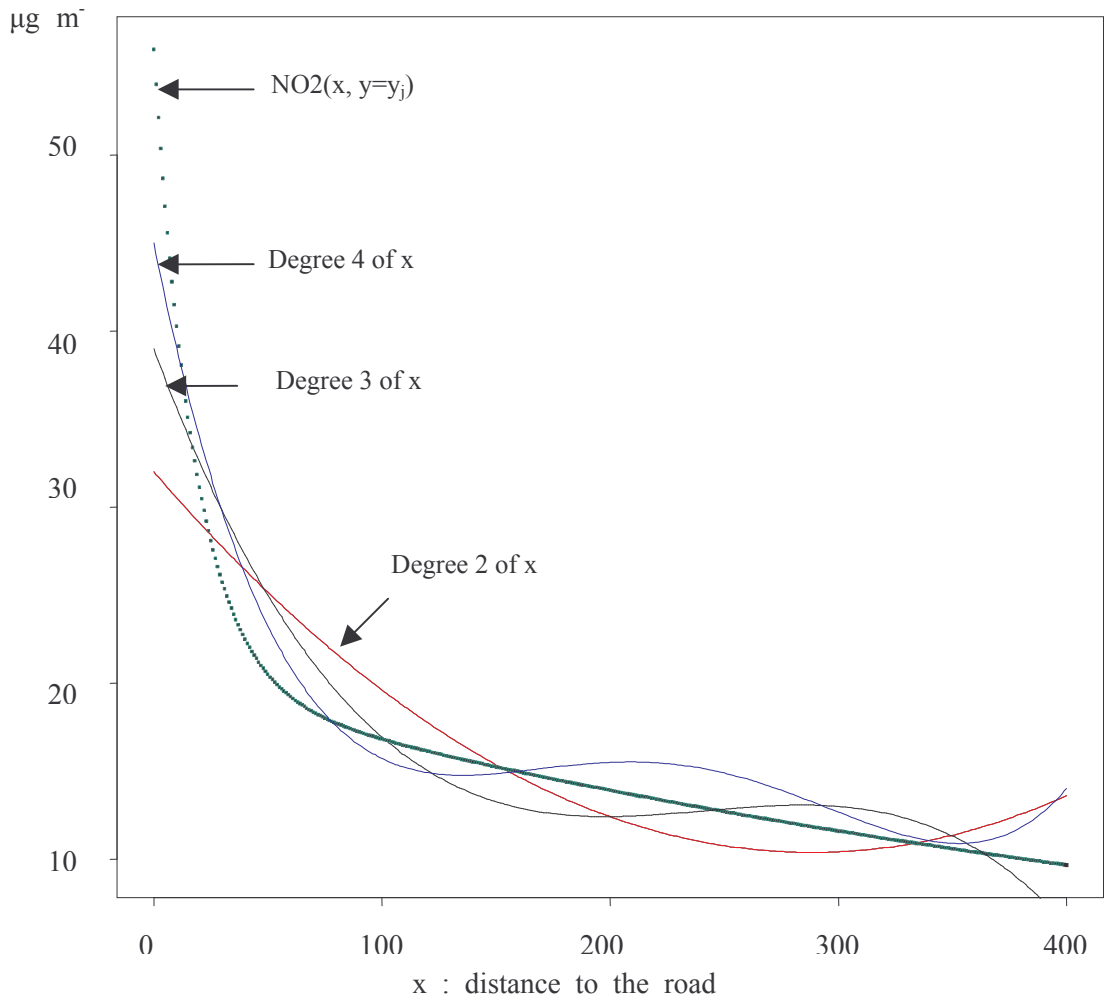
µg m-
NO2(x, y=yj)
Degree 4 of x
Degree 3 of x
Degree 2 of x
50
40
30
20
10
0
100
200
300
400
x : distance to the road

419 Fig. 7

420